

## Electronic supplementary information

### Pure Red Emission with Spectra-Stable in Full Iodine-based Quasi-2D Perovskite Films by Controlling Phase Distribution

Zhiqiang Ming,<sup>a</sup> Siyao Li,<sup>a</sup> Xinyi Luo,<sup>a</sup> Siman Liu,<sup>a</sup> Danliang Zhang,<sup>a</sup> Xiaoli Zhu,<sup>a</sup> Anlian Pan,<sup>a</sup> and Xiao Wang<sup>\*a</sup>

<sup>a</sup> School of Physics and Electronics, Key Laboratory for Micro-Nano Physics and Technology of Hunan Province, and College of Materials Science and Engineering, Hunan University, Changsha 410082, China  
E-mail: xiao\_wang@hnu.edu.cn

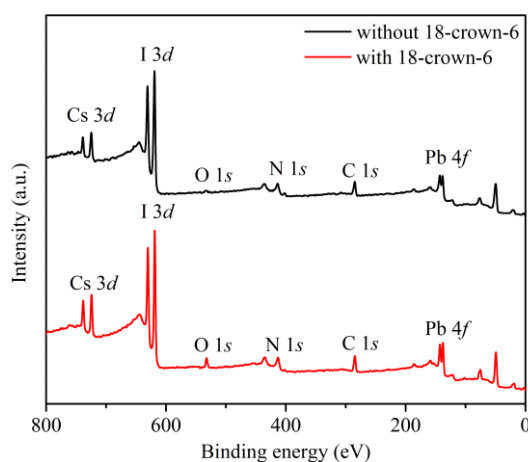


Fig. S1 XPS spectra of quasi-2D perovskite films without and with 18-crown-6.

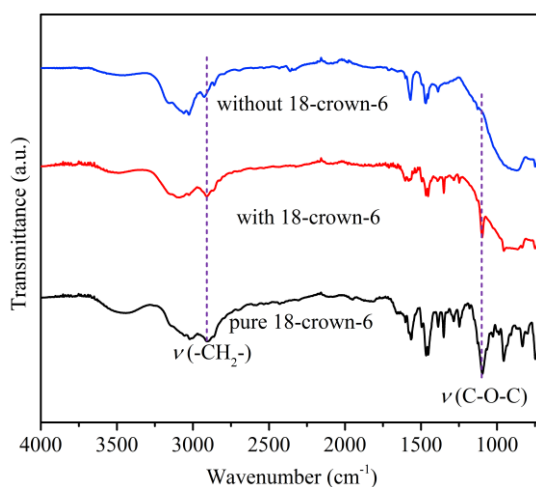


Fig. S2 FTIR spectra of quasi-2D perovskite films without and with 18-crown-6 in comparison with the pure 18-crown-6.

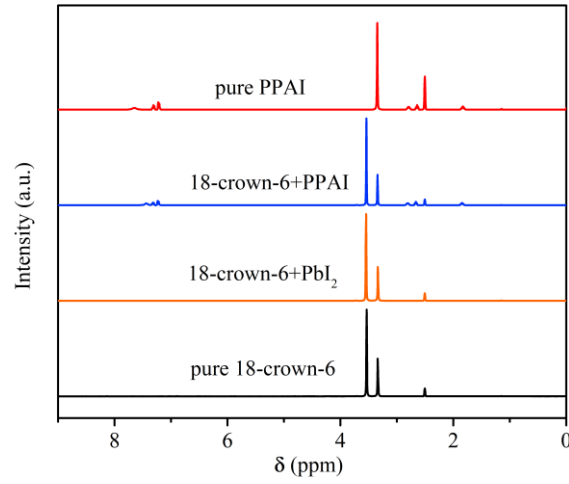


Fig. S3  $^1\text{H}$  NMR spectra of pure 18-crown-6, 18-crown-6 with  $\text{PbI}_2$ , 18-crown-6 with PPAI and pure PPAI in deuterated DMSO.

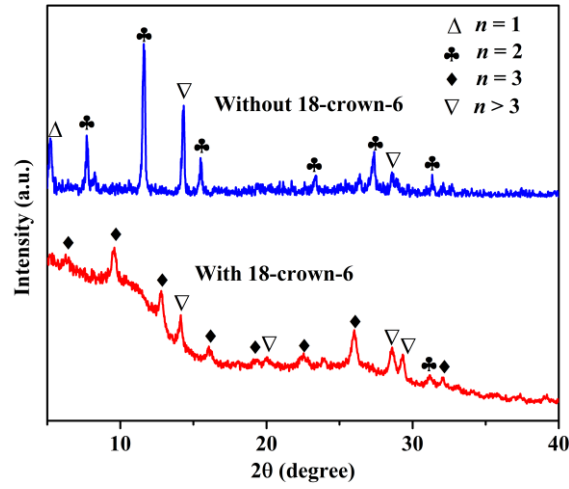


Fig. S4 GIXRD spectra of quasi-2D perovskite films without and with 18-crown-6. The film without 18-crown-6 exhibited typical diffraction peaks with  $2\theta$  periodicity of  $3.9^\circ$ , corresponding to (0k0) reflections. We calculated the d-spacing was about 2.26 nm, which was similar to  $\text{BA}_2\text{MAPb}_2\text{I}_7$ .<sup>1</sup> Thus, we attributed above diffraction peaks (0k0) to  $n = 2$  perovskite. Similarly, the film with 18-crown-6 exhibited typical diffractions with  $2\theta$  periodicity of  $3.2^\circ$ , corresponding to (0k0) reflections. We calculated the d-spacing was about 2.76 nm, similar to  $\text{BA}_2\text{MA}_2\text{Pb}_3\text{I}_{10}$ .<sup>2</sup> Thus, these diffraction peaks could be ascribed to  $n = 3$  perovskite crystal planes.

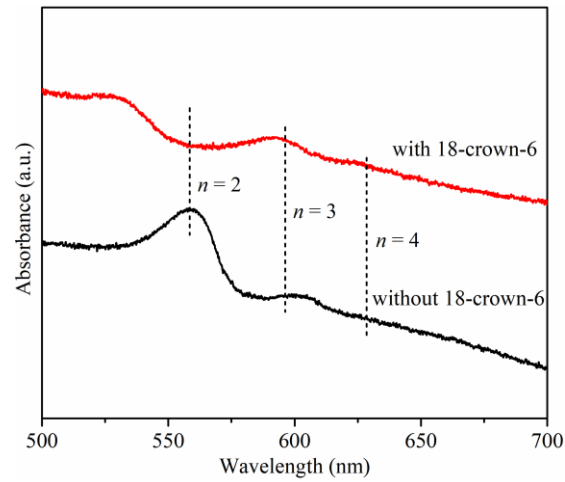


Fig. S5 UV-vis absorption spectra of perovskite films without and with adding 18-crown-6 additions.

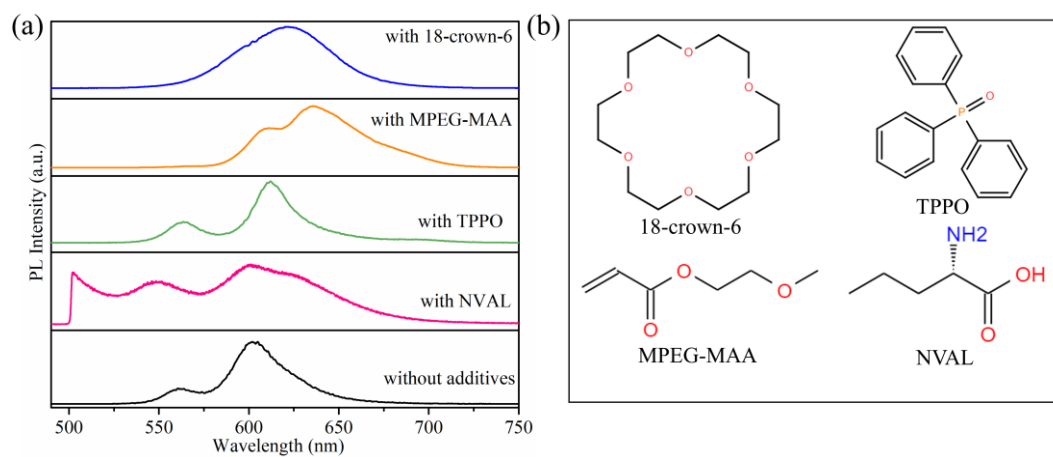


Fig. S6 (a) Log PL spectra of perovskite films without and with various types of additives under 488 nm excitation. (b) The molecular structure of various additives including 18-crown-6, poly(ethylene glycol)methyl ether acrylate (MPEG-MAA), triphenylphosphine oxide (TPPO) and L-Norvaline (NVAL).

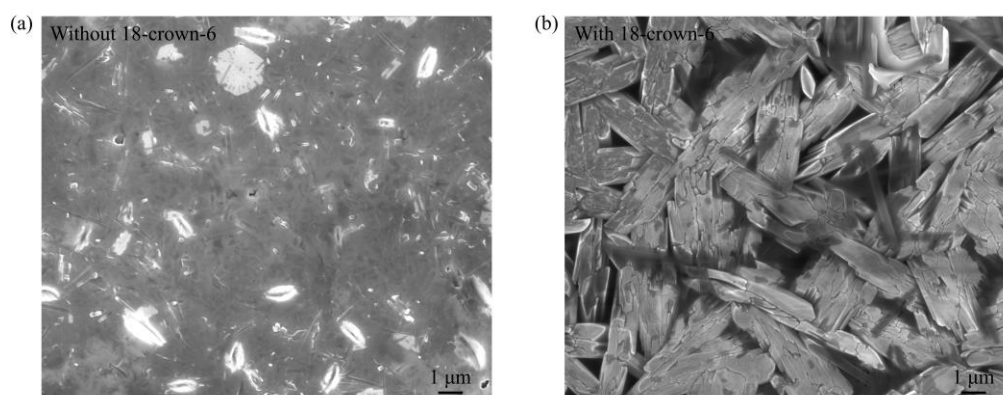


Fig. S7 Top-view SEM images of perovskite films without (a) and with (b) 18-crown-6 additives.

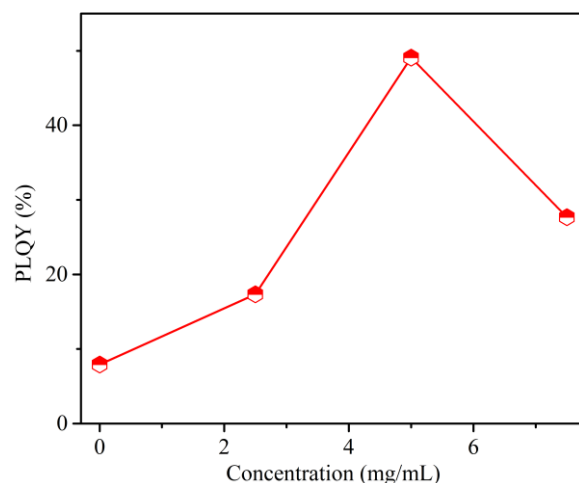


Fig. S8 PLQY of perovskite films with adding various contents of 18-crown-6.

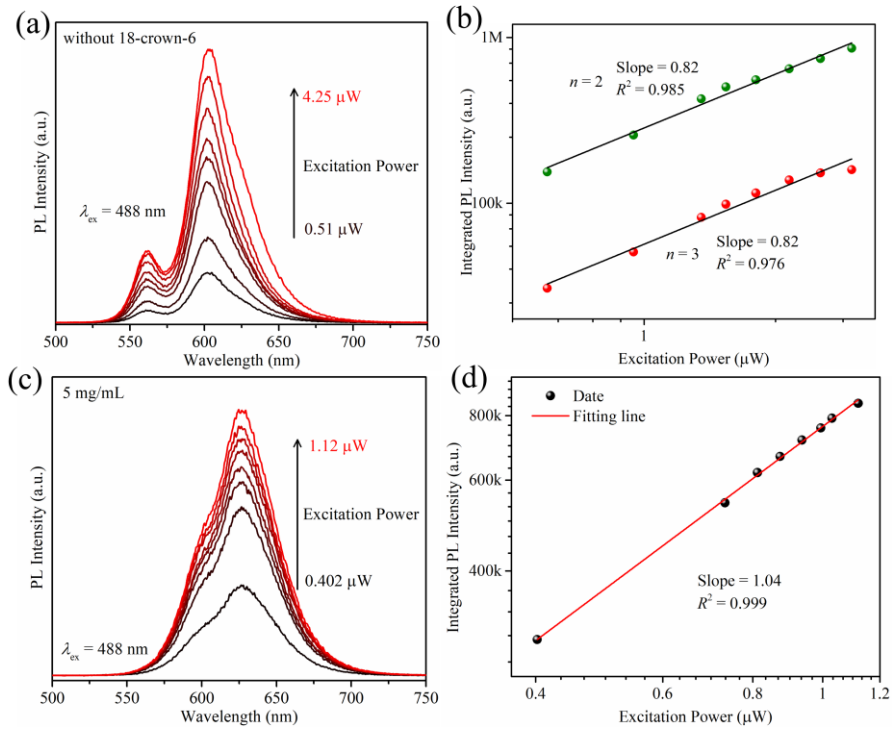


Fig. S9 Perovskite films with adding various contents of 18-crown-6: (a) (d) power dependent PL spectra, and (b) (c) PL intensity of emission peak under varying excitation power.

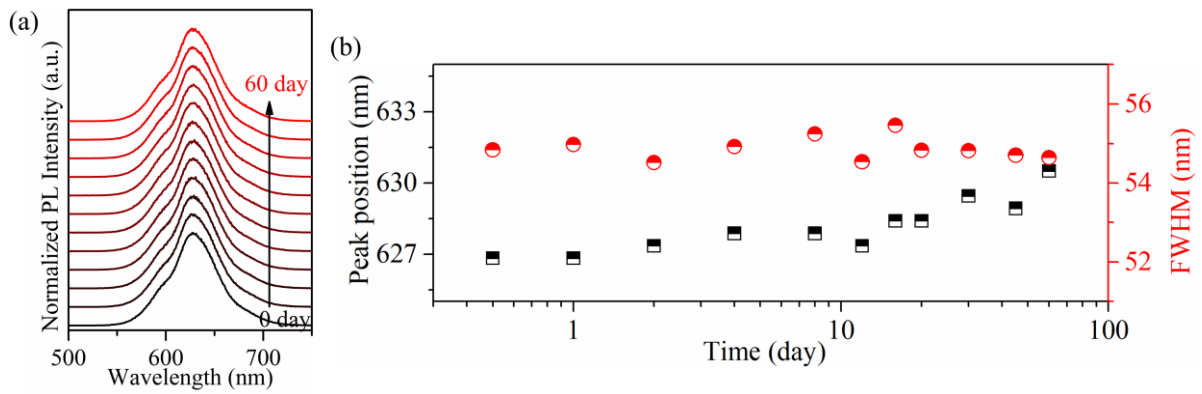


Fig. S10 (a) PL spectra and (b) corresponding the FWHM and peak position difference of quasi-2D perovskite films with 18-crown-6 after exposure to air for 0-60 days.

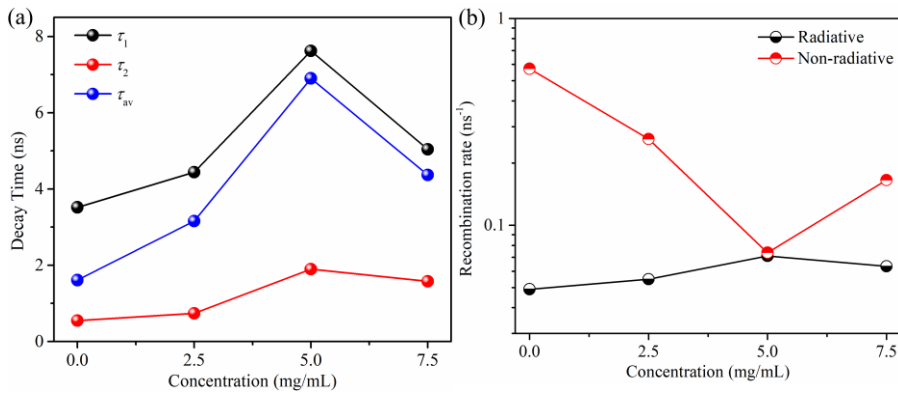


Fig. S11 (a) Slow decay lifetime  $\tau_1$ , fast decay lifetime  $\tau_2$  and average decay lifetime  $\tau_{\text{av}}$  (b) radiative and non-radiative recombination rate of perovskite films without and with adding various concentration of 18-crown-6 additions.

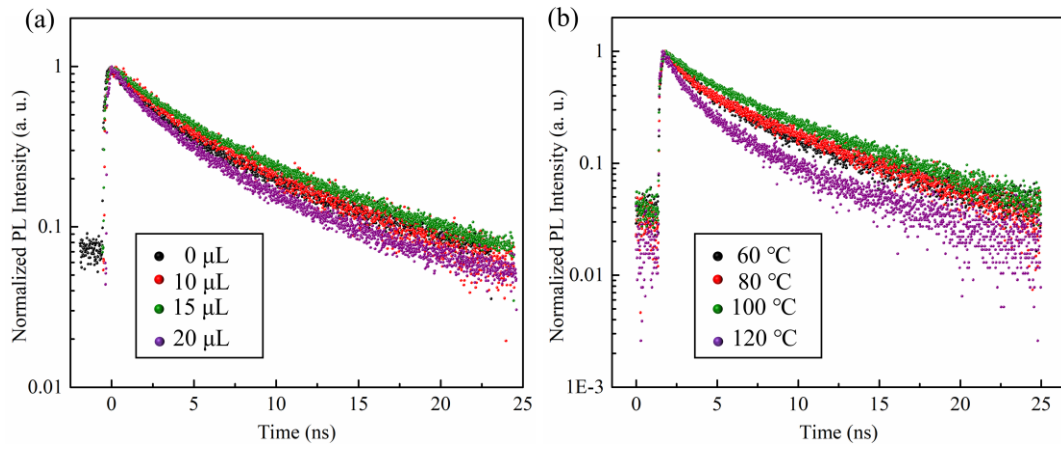


Fig. S12 TRPL decay curves of quasi-2D perovskite films with (a) various contents of CB and (b) different annealing temperature under 405 nm irradiation.

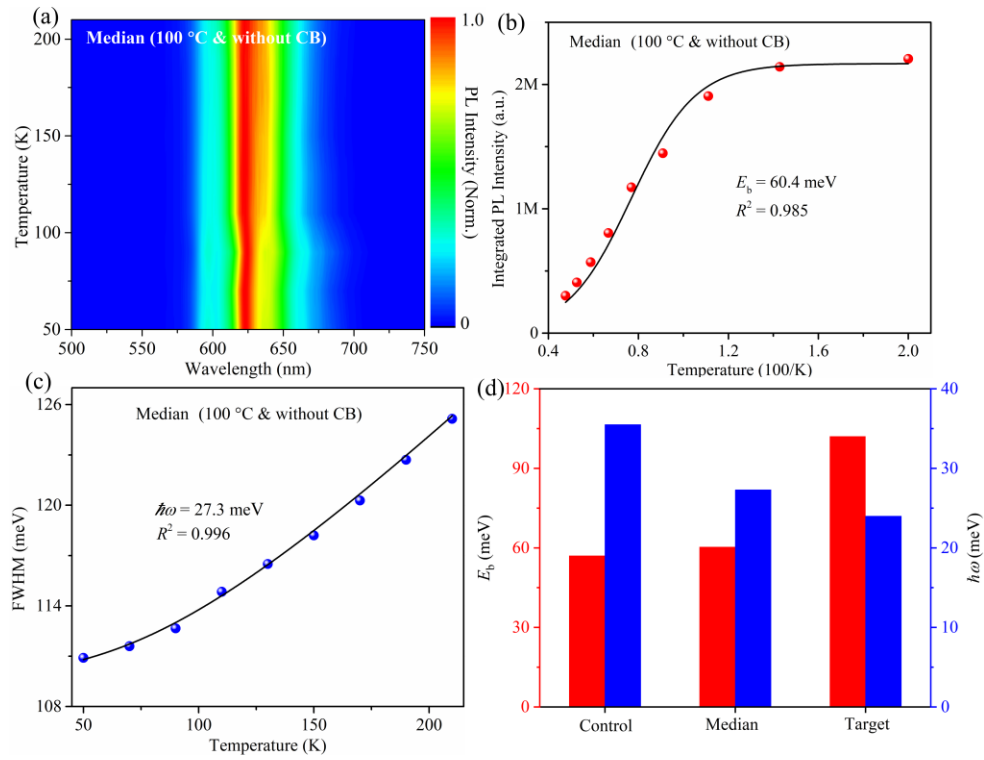


Fig. S13 Normalized temperature-dependent PL spectra of (a) median perovskite film (with annealing at 100 °C and without CB). (b) Relevant integration of PL intensity of median film and fitting curve for  $E_b$ . (c) FWHM of pure red emission peak as a function of temperature of median film. (d) Comparison of exciton binding energy ( $E_b$ ) and longitudinal optical phonon energy ( $\hbar\omega$ ) in different samples.

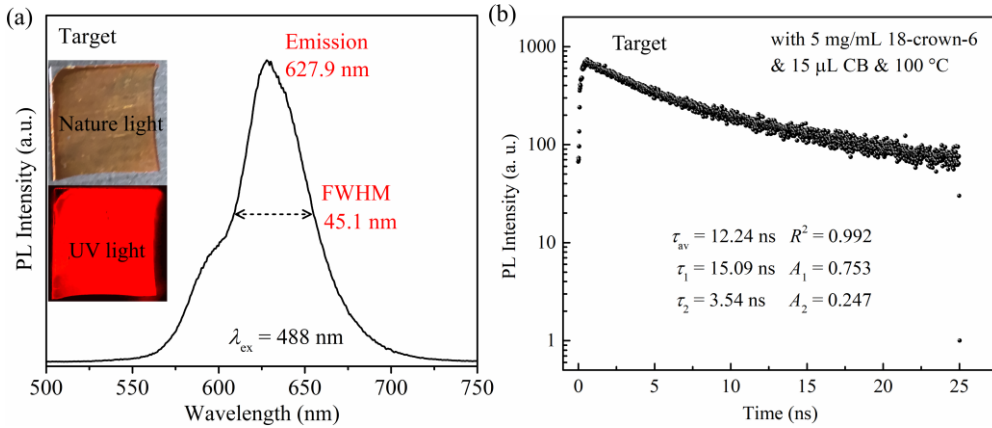


Fig. S14 (a) PL and (b) TRPL decay curve of target quasi-2D perovskite films under 405 nm irradiation.

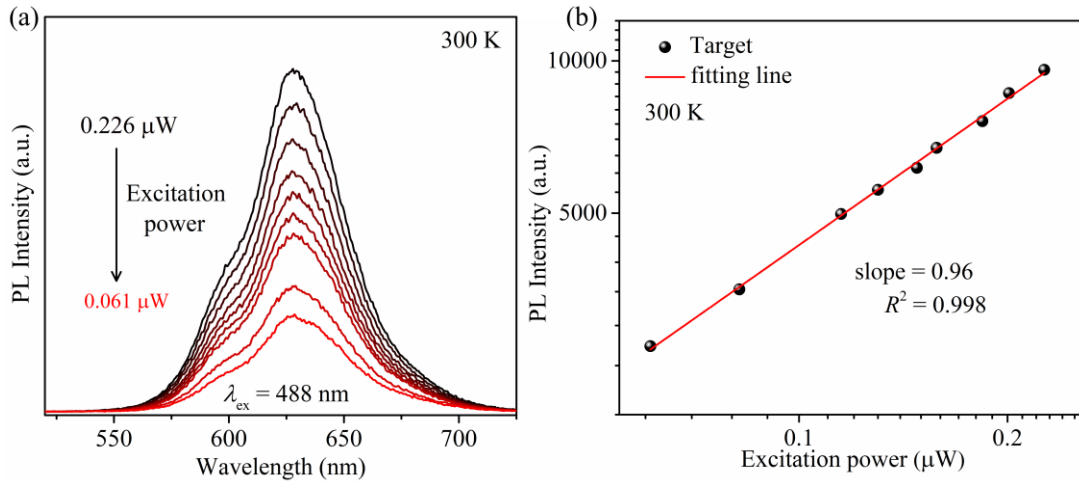


Fig. S15 (a) Power dependent PL spectra of optimized quasi-2D perovskite films under varying excitation power. (b) PL intensity of emission peak under varying excitation power.

#### Note S1

All PL decay curves could be well fitted by a bi-exponential decay function:  $I(t) = A_1 \exp(-t/\tau_1) + A_2 \exp(-t/\tau_2)$ , where  $A_1$  and  $A_2$  are constant,  $\tau_1$  and  $\tau_2$  are the slow decay lifetime of corresponding radiation recombination and the fast decay lifetime of corresponding non-radiation recombination.<sup>3</sup> The average lifetime is calculated using the equation:  $\tau_{\text{av}} = (A_1 \tau_1^2 + A_2 \tau_2^2) / (A_1 \tau_1 + A_2 \tau_2)$ . Based on results of PLQY and decay lifetime, we calculated the radiative and non-radiative recombination rate ( $k_r$ ,  $k_{nr}$ ) of films using the equation of  $\text{PLQY} = k_r / (k_r + k_{nr})$ ,  $\tau_{\text{av}} = 1 / (k_r + k_{nr})$ .

#### Note S2

All temperature-dependent integration of PL intensity of target and control films curves could be well fitted by Arrhenius equation:  $I(T) = I_0 / (1 + A \exp(-E_b/kT))$ , in which  $I(T)$  and  $I_0$  are the integrated PL intensity under the temperature of T K and 0 K,  $k$  is the Boltzmann constant, and  $E_b$  is the exciton binding energy.<sup>4</sup>

#### Note S3

The broadening emission band with increasing temperature could be fitted based on the independent Boson model:  $I(T) = \Gamma_0 + \sigma T + \Gamma_{\text{op}} / (\exp(\hbar\omega/kT) - 1)$ , where  $\Gamma_0$  represents the temperature-independent inhomogeneous broadening, the other terms represent the homogeneous broadening, attributing to the exciton-acoustic phonon interaction ( $\sigma$ ) and the exciton-longitudinal optical phonon interaction ( $\Gamma_{\text{op}}$ ).<sup>5</sup>

**Table S1.** Progress of pure red full iodine-based quasi-2D perovskite films.

Composition	Difference of pure red peak position (nm)	FWHM (nm)	Reference
$(\text{PBA}_x\text{MBZA}_{1-x})_2\text{CS}_{n-1}\text{PbI}_{3n+1}$ ( $x = 1$ )	4	49	[6]
$(\text{PBA}_x\text{MBZA}_{1-x})_2\text{CS}_{n-1}\text{PbI}_{3n+1}$ ( $x = 0.75$ )	2	49	[6]
$(\text{PBA}_x\text{MBZA}_{1-x})_2\text{CS}_{n-1}\text{PbI}_{3n+1}$ ( $x = 0.5$ )	9	47	[6]
$(\text{PBA}_x\text{MBZA}_{1-x})_2\text{CS}_{n-1}\text{PbI}_{3n+1}$ ( $x = 0.25$ )	20	42	[6]
$(\text{PBA}_x\text{POEA}_{1-x})_2\text{CS}_{n-1}\text{PbI}_{3n+1}$ ( $x = 0.75$ )	1	46	[6]
$(\text{PBA}_x\text{POEA}_{1-x})_2\text{CS}_{n-1}\text{PbI}_{3n+1}$ ( $x = 0.5$ )	6	45	[6]
$(\text{PBA}_x\text{POEA}_{1-x})_2\text{CS}_{n-1}\text{PbI}_{3n+1}$ ( $x = 0.25$ )	10	42	[6]
$(\text{PBA}_x\text{POEA}_{1-x})_2\text{CS}_{n-1}\text{PbI}_{3n+1}$ ( $x = 0$ )	12	41	[6]
$(\text{POEA}_x\text{MBZA}_{1-x})_2\text{CS}_{n-1}\text{PbI}_{3n+1}$ ( $x = 0.75$ )	15	38	[6]
$(\text{POEA}_x\text{MBZA}_{1-x})_2\text{CS}_{n-1}\text{PbI}_{3n+1}$ ( $x = 0.5$ )	20	38	[6]
$(\text{PEA}_{0.5}\text{NMA}_{0.5})_2\text{CsPbI}_7$	5	46	[7]
$\text{PEA}_2(\text{Cs}_{0.3}\text{MA}_{0.7})_2(\text{Pb}_{1-x}\text{Zn}_x)_3\text{I}_{10}$ ( $x = 0.45$ )	7	61	[8]
$\text{BA}_2\text{CS}_{n-1}\text{PbI}_{3n+1}$ (No.2)	4	55	[9]
$\text{PBA}_2\text{CS}_{n-1}\text{PbI}_{3n+1}$ ( $\text{PBA}_1\text{PI}$ )	13	48	[10]
$\text{PPA}_2\text{CS}_{n-1}\text{PbI}_{3n+1}$	20	46	[11]
$\text{POEA}_2\text{CsPbI}_7$	15	45	[12]
$(\text{PEA}/\text{NMA})_2\text{CS}_{n-1}\text{PbI}_{3n+1}$	18	47	[13]
$(\text{PEA}/\text{PBA}/\text{NMA})_2\text{CS}_{n-1}\text{PbI}_{3n+1}$	3	48	[14]
<b><math>\text{PPA}_2\text{CS}_{n-1}\text{PbI}_{3n+1}</math> (This work)</b>	<b>2.1</b>	<b>45.1</b>	-

## Reference

- [1] M. C. Weidman, M. Seitz, S. D. Stranks and W. A. Tisdale, *ACS Nano*, 2016, **10**, 7830-7839.
- [2] C. C. Stoumpos, D. H. Cao, D. J. Clark, J. Young, J. M. Rondinelli, J. I. Jang, J. T. Hupp and M. G. Kanatzidis, *Chem. Mater.*, 2016, **28**, 2852-2867.
- [3] P. Liu, W. Cai, C. Zhao, S. Zhang, P. Nie, W. Xu, H. Meng, H. Fu and G. Wei, *Adv. Optic. Mater.*, 2021, **9**, 2101419.
- [4] F. Zhao, H. W. Duan, S. N. Li, J. L. Pan, W. S. Shen, S. M. Li, Q. Zhang, Y. K. Wang and L. S. Liao, *Angew. Chem. Int. Ed.*, 2023, **62**, e202311089.
- [5] H. Li, H. Lin, D. Ouyang, C. Yao, C. Li, J. Sun, Y. Song, Y. Wang, Y. Yan, Y. Wang, Q. Dong and W. C. H. Choy, *Adv. Mater.*, **2021**, **33**, e2008820.
- [6] J. Qing, S. Ramesh, Q. Xu, X. K. Liu, H. Wang, Z. Yuan, Z. Chen, L. Hou, T. C. Sum and F. Gao, *Adv. Mater.*, 2021, **33**, e2104381.
- [7] L. Yang, Y. Zhang, J. Ma, P. Chen, Y. Yu and M. Shao, *ACS Energy Lett.*, 2021, **6**, 2386.
- [8] D. Liu, X. Liu, G. Sun, F. Meng, Z. Liu, C. Shen, M. Li and S. J. Su, *ACS Appl. Mater. Interfaces*, 2021, **13**, 55412.
- [9] Y. Tian, C. Zhou, M. Worku, X. Wang, Y. Ling, H. Gao, Y. Zhou, Y. Miao, J. Guan and B. Ma, *Adv. Mater.*, 2018, **30**, e1707093.
- [10] Z. He, Y. Liu, Z. Yang, J. Li, J. Cui, D. Chen, Z. Fang, H. He, Z. Ye, H. Zhu, N. Wang, J. Wang and Y. Jin, *ACS Photonics*, 2019, **6**, 587.
- [11] J. Qing, S. Ramesh, X. Liu, H. Wang, H. Yu, C. Kuang, L. Hou, W. Zhang, T. C. Sum and F. Gao, *Applied Surface Science*, 2023, **616**, 156454.
- [12] Y. Kuang, L. Yang, J. Ma, T. Bie, D. Zhang, Y. Xue, N. Zhou and M. Shao, *ACS Mater. Lett.*, 2023, **5**, 2922.
- [13] S. Liu, H. Zhan, C. Qin and C. Qin, *J. Phys. Chem. Lett.*, 2023, **14**, 73.
- [14] S. Liu, H. Zhan, C. Qin and C. Qin, *Chemical Engineering Journal*, 2024, **479**, 147866.